

# Design of Intrinsically Flame-Retardant Vanillin-Based Epoxy Resin for Thermal-Conductive Epoxy/Graphene Aerogel Composites

Weijun Yang,\* Hui Ding, Tianxi Liu, Rongxian Ou, Jieying Lin, Debora Puglia, Pengwu Xu, Qingwen Wang, Weifu Dong, Mingliang Du, and Piming Ma\*



Cite This: *ACS Appl. Mater. Interfaces* 2021, 13, 59341–59351



Read Online

ACCESS |



Metrics & More



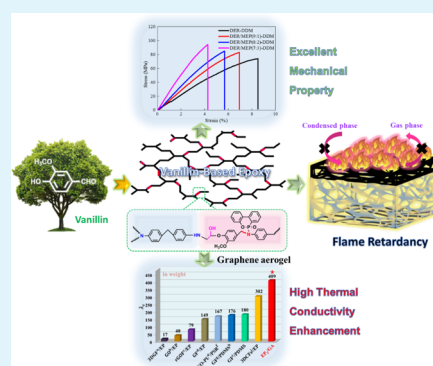
Article Recommendations



Supporting Information

**ABSTRACT:** Vanillin, as a lignin-derived mono-aromatic compound, has attracted increasing attention due to its special role as an intermediate for the synthesis of different biobased polymers. Herein, intrinsically flame-retardant and thermal-conductive vanillin-based epoxy/graphene aerogel (GA) composites were designed. First, a bifunctional phenol intermediate (DN-bp) was synthesized by coupling vanillin with 4, 4'-diaminodiphenylmethane and DOPO, and the epoxy monomer (MEP) was obtained by the epoxidation reaction with DN-bp and epichlorohydrin. Then, various amounts of MEP and diglycidyl ether of bisphenol A (DER) were mixed and cured. Interestingly, the flexural strength and modulus were greatly enhanced from 72.8 MPa and 1.3 GPa to 90.3 MPa and 2.8 GPa, respectively, at 30 wt % MEP, due to the rigidity of MEP and strong intermolecular N–H hydrogen bonding interactions. Meanwhile, the cured epoxy achieved a UL-94 V0 rating with a low P content of 1.06%. The flame-retardant vanillin-based epoxy was then impregnated into the thermal conductive 3D GA networks. The obtained epoxy/graphene composite showed excellent flame retardancy and thermal conductivity [ $\lambda = 0.592 \text{ W}/(\text{m}\cdot\text{K})$ ] with only 0.5 wt % graphene in the system. Based on these results, we believe that this work would represent a novel solution for the preparation of high-performance biobased flame-retardant multipurpose epoxies.

**KEYWORDS:** vanillin, epoxy resin, flame retardancy, thermal conductivity, graphene aerogels



## 1. INTRODUCTION

Thermosetting polymers have been extensively considered for applications in different sectors, such as aerospace,<sup>1</sup> electronics,<sup>2</sup> high-performance composites,<sup>3,4</sup> and coatings.<sup>5</sup> Epoxy resins (EP) have tremendous potential utilization, due to their excellent dimensional stability, chemical resistance, and balanced mechanical performances. Nevertheless, most of commercial EPs are obtained by petroleum resources, and 90% EPs are represented by diglycidyl ether of bisphenol A (DGEBA), which are prepared from bisphenol A and epichlorohydrin (ECH).<sup>6</sup> Additionally, bisphenol A is mostly produced using petroleum resources that also exacerbate environment issues. Hence, the preparation of polymeric materials from biomass feedstock is a vital strategy to replace petroleum-based resources.

In the past two decades, biobased EPs have been considered to replace fossil-based alternatives:<sup>7</sup> until now, plenty of bio-renewable feedstock materials, such as epoxidized soybean oils,<sup>8,9</sup> itaconic acid,<sup>10</sup> cardanol,<sup>11,12</sup> and lignin<sup>13–16</sup> and its derivatives,<sup>17–19</sup> have aroused much attention for the preparation of EPs. Although great progress has been made in the preparation of these bio-renewable products, the comprehensive properties of EPs are limited, owing to the specific chemical structure and limited storages of bio-

renewable raw materials. Therefore, the preparation of biobased EPs with excellent and stable properties has generated great impact.

It is well-known that conventional fossil-based EPs have inherent drawbacks in terms of flammability property, which hinder EPs from being utilized in some specific fields requiring fire resistance.<sup>20–22</sup> In order to overcome the shortcoming mentioned above, it is indispensable to modify EPs to enhance their flame resistance performances. Differently from traditional halogenated flame retardants, flame retardants containing phosphorous, for instance 9,10-dihydro-9-oxo-10-phosphaphenanthrene-10-oxide (DOPO), various phosphates, and phosphonitrilic chloride trimer,<sup>19,23–26</sup> have gained great popularity in contemporary society since they exhibit non-toxic, environmental friendly, and renewable properties during combustion. Among them, DOPO has gained much favor within researchers, owing to high reactivity and low cost.<sup>27</sup>

**Received:** October 12, 2021

**Accepted:** November 23, 2021

**Published:** December 3, 2021



Recently, for the sake of enhancing the flame retardancy efficiency, adding phosphorus (P) and nitrogen (N) into the EP matrix in a synergic manner has been considered to be one of the most effective and ecofriendly approach for flame retardants. For example, Guo et al.<sup>28</sup> reported about the preparation of a novel flame-retardant and highly toughened EP that exhibited higher limited oxygen index (LOI) value (~33.5%), UL-94 V0 rating, and lower peak heat release rate (PHRR) (~301 kW/m<sup>2</sup>) than commercial EP. Additionally, the novel cured EP possessed good toughness.

Vanillin, as lignin derivative, is a renewable and abundant mono aromatic compound with enormous potential for the preparation of biobased polymers, such as EPs.<sup>29–31</sup> Ma et al.<sup>18</sup> reported about the preparation of vanillin-based phosphate EPs with excellent fire resistance and extremely high  $T_g$  (~214 °C). The LOI of cured EP was up to 32.8, and the UL-94 reached V0 rating. However, additive flame retardants, especially P containing flame retardants, may affect the mechanical properties of polymers.<sup>32</sup>

In order to expand the application fields of EP, some other properties should also be taken into consideration, such as thermal conductivity, heat resistance, electromagnetic shielding, wave absorption, and transmission.<sup>33–36</sup> Especially in the case of electronic packaging fields, the fire resistance performance of EPs has been deemed to be insufficient, and the poor thermal conductivity would seriously threaten personal safety and property loss.<sup>37,38</sup> Consequently, preparation of flame-retardant EPs with enhanced thermal conductivity has become a significant and preventive measure. Gu et al.<sup>39</sup> reported about the preparation of a novel P- and N-based flame-retardant epoxy nanocomposite containing functional graphite nanoplatelet fillers: they showed that the modified epoxy nanocomposite had a high LOI value (~37%) and possessed excellent thermal conductivity, which was 700% higher than neat flame-retardant EP. Feng et al.<sup>40</sup> studied the thermal conductivity and flame retardancy of EP composites using DOPO-decorated reduced graphene oxide (rGO) as a flame-retardant unit and silver nanowires (AgNWs) and DOPO-modified rGO as thermal conductive units, by obtaining values for thermal conductivity approximately five times higher than neat EP.

Thus, in this study, we designed and synthesized a highly efficient bio-based flame-retardant epoxy monomer (MEP) from lignin-derived vanillin, 4,4'-diaminodiphenylmethane (DDM), and DOPO and thermal-conductive epoxy/graphene aerogel (GA) composites. First, the flame-retardant bifunctional phenol intermediate (DN-bp) was obtained via a one-pot and green approach: (1) the Schiff base compound was synthesized from vanillin and DDM; (2) the P–H of DOPO reacted with the Schiff base by the addition reaction without purification. Then, the MEP was obtained by the reaction of DN-bp and ECH. The obtained MEP was then characterized for its chemical structure, and curing behavior, flexural performance, flame retardancy mechanism, and thermal stability of different DGEBA (DER)-based formulations containing various amounts of MEP were evaluated. With the aim of evaluating the effective use of produced biobased EPs even when thermal conductivity is required, the studied flame-retardant EP was considered for the vacuum impregnation of a 3D graphene oxide/polyvinyl alcohol (PVA) aerogel network (GA). We considered this approach as a green and ecofriendly solution for the replacement of petroleum-based

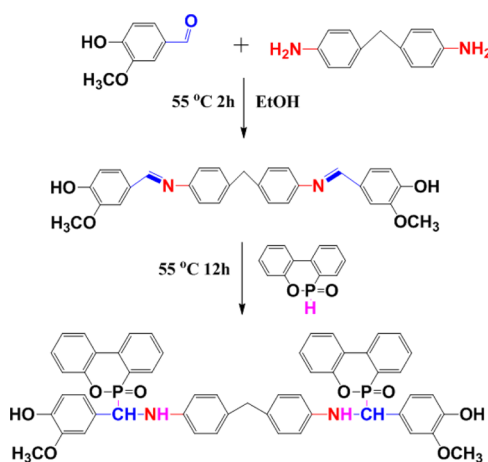
EP by biobased flame-retardant formulations in bulk and thermally conductive aerogel systems.

## 2. EXPERIMENTAL SECTION

**2.1. Materials.** Vanillin was purchased from Shanghai Macklin Biochem Co., Ltd. DDM (>98.5% purity), DOPO (97% purity), ECH (99% purity), tetrabutylammonium bromide (TBAB, 99% purity), NaOH, and all the required chemicals/organic solvents were purchased from Sinopharm Chemical Reagent Co., Ltd. Epoxy resin (DGEBA, trade name DER, epoxy equivalent value 0.52–0.54 g/eq) was purchased from Shanghai Kaiyin Co., Ltd. Graphene oxide (GO) (99% purity, <80 mesh) was provided by Sui Heng Technology Co., Ltd. (Shenzhen, China). PVA ( $M_w = 120–150 \text{ kg}\cdot\text{mol}^{-1}$ ) was purchased from Sigma-Aldrich.

**2.2.1. Preparation of Di-phenol Intermediate (DN-bp).** The synthesis of DN-bp was performed via a facile condensation reaction, as presented in Scheme 1: vanillin (30.44 g, 0.2 mol) was dissolved in

**Scheme 1. Synthesis Routes of DN-bp**



ethyl alcohol (100 mL) in a three-neck flask assembled under a nitrogen atmosphere with a magnetic stirrer and a reflux condenser. DDM (19.84 g, 0.1 mol), dissolved in ethyl alcohol (100 mL), was added dropwise into the flask at 55 °C for 30 min and then maintained at 55 °C for 2 h. Afterward, DOPO powder (43.24 g, 0.2 mol) was incorporated into the mixture and sequentially maintained at 55 °C for 12 h. The reaction was naturally cooled to room temperature. After that, the mixture was dissolved in dichloromethane and then poured into ethyl alcohol. Finally, the DN-bp product was obtained by filtration, dried overnight at 80 °C in the vacuum oven. DN-bp: light yellow solid, yield 87.4 wt %.

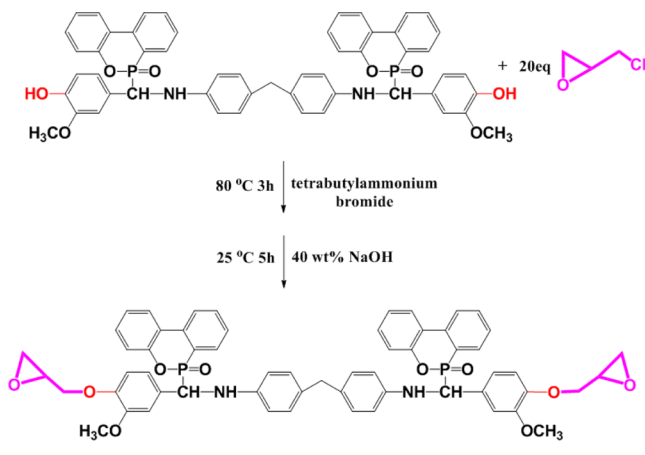
<sup>1</sup>H NMR (400 MHz, DMSO)  $\delta = 3.46$  (d, 1H), 3.64 (d, 3H), 4.87 (m, 1H), 5.23 (m, 1H), 6.04 (s, 1H), 6.41 (d, 1H), 6.58–6.49 (m, 3H), 8.05–6.87 (m, 8H), 8.21–8.12 (m, 2H), 8.91 (d, 1H).

**2.2.2. Preparation of the Epoxy Monomer (MEP).** The MEP was synthesized by following the epoxidation reaction, as reported in Scheme 2. Under magnetic stirring, DN-bp (17.98 g, 0.02 mol) and ECH (37.00 g, 0.4 mol) were incorporated into a three-neck flask with constant stirring. After that DN-bp was completely dissolved, TBAB (1.65 g) as a catalyst was added at 80 °C for 3 h. Then, the reaction was cooled to 50 °C, and 40 wt % NaOH (1.6 g, 0.04 mol) aqueous solution was added dropwise for 20 min. The reaction was kept for another 3 h, afterward being cooled to room temperature.

The crude product was dissolved in dichloromethane and then washed with distilled water for three times to remove the salt. Finally, organic solvent was removed using the rotary evaporator, and the obtained product was dried overnight at 80 °C under a vacuum oven. MEP: light yellow oil, yield 92.5 wt %.

<sup>1</sup>H NMR (400 MHz, DMSO)  $\delta = 2.62$  (dd, 2H), 2.81 (t, 2H), 2.96 (s, 2H), 3.18 (s, 2H), 3.49 (m, 3H), 3.61 (m, 4H), 3.92 (m, 2H), 6.04 (s, 1H), 6.32 (d, 1H), 6.58–6.49 (m, 4H), 8.05–6.87 (m, 10H).

Scheme 2. Synthesis Routes for MEP



**2.3. Preparation of the Cured Epoxy Systems.** EPs of DER and MEP [mass ratios 10:0, 9:1, 8:2, and 7:3, named as DER-DDM, DER/MEP (9:1)-DDM, DER/MEP (8:2)-DDM, and DER/MEP (7:3)-DDM] were cured with DDM (a molar ratio of N–H to the epoxy group was 1:1). The formulations are reported in Table S1. The mixtures were fully stirred at 80 °C to get homogeneous systems, degassed under vacuum to remove the bubbles, and then poured into a preheated stainless-steel mold for the curing process: 80, 120, and 160 °C for 2 h each step. Finally, the samples were cooled to room temperature and removed from the mold.

**2.3.1. Preparation of EP/Graphene Composites.** The preparation of GA is supplied in the Supporting Information. EP/GA composites were prepared by the vacuum impregnation method. First, EP and curing agent DDM were mixed at 80 °C. The GA aerogels were first impregnated with the EP mixture and then maintained under vacuum condition until no bubbles escaped on the sample surface. Subsequently, the samples were cured in the oven at 80 °C for 2 h, 120 °C for 2 h, and 160 °C for 2 h, respectively. DER-DDM is named as EP<sub>1</sub>, and DER/MEP (8:2) is denoted as EP<sub>2</sub> (more details are available in the Supporting Information).

**2.4. Characterizations.** The performed characterizations of the flame-retardant epoxy and epoxy/graphene composites are available in the Supporting Information.

### 3. RESULTS AND DISCUSSION

**3.1. Synthesis and Characterization of DN-bp and MEP.** Scheme 1 illustrates the synthesis of DN-bp through a facile one-pot procedure from bio-renewable feedstock vanillin, DDM, and DOPO. First, the Schiff-based intermediate was prepared through the condensation reaction between the aldehyde group of vanillin and amino group of DDM.<sup>18</sup> Then, the intermediate DN-bp was obtained through the phosphorus–hydrogen addition reaction with DOPO without purification. In Scheme 2, the bio-renewable epoxy monomer was prepared via the glycidyl etherification reaction between DN-bp and ECH.<sup>41</sup> The FTIR spectra of vanillin, DOPO, DN-bp, and MEP are reported in Figure 1. In the vanillin spectrum, the peaks at 3100–3500 and 1665 cm<sup>-1</sup> belong to –OH and stretching vibration of C=O, respectively. The peak at 1665 cm<sup>-1</sup> of the C=O bond, and the peak at 2438 cm<sup>-1</sup> of P–H disappear in DN-bp. The broad characteristic peak at 3100–3600 cm<sup>-1</sup> corresponds to the –OH and N–H, and the peaks of P–C, C–N, P=O, and P–O appear at about 1600, 1280, 1240, and 926 cm<sup>-1</sup>, respectively.<sup>42,43</sup> In MEP spectrum, a new weak peak belonging to the epoxy group appears at 905 cm<sup>-1</sup>, proving the successful synthesis of the MEP epoxy monomer. The H signals are elucidated in Figure 2a<sub>1</sub>,b<sub>1</sub>, demonstrating

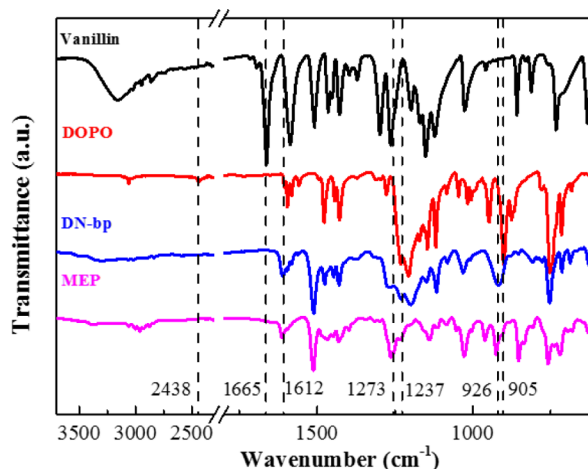


Figure 1. FTIR spectra of vanillin, DOPO, DN-bp, and MEP.

the chemical structure of DN-bp and MEP. Additionally, two unequal phosphorus signals at 28.9 and 31.5 ppm are observed in Figure 2a<sub>2</sub>,b<sub>2</sub> because of the steric hindrance effects of DOPO.<sup>42,44</sup> In order to further confirm the chemical structures of DN-bp and MEP, the <sup>13</sup>C NMR spectra are also displayed in Figure S2. According to the above discussion, the DN-bp and MEP were successfully prepared.

**3.2. Curing Behavior.** In order to analyze the effect of MEP introduction on curing behavior of epoxy systems, the different DER/MEP-DDM epoxy systems were investigated at various heating rates. Notably, all cured epoxy systems showed one single curing exothermic peak. It is well known that lower peak temperature means higher reactivity.<sup>45</sup> As shown in Figure 3a–d, it is visible that the peak temperature of the DER/MEP-DDM systems exhibited a declining trend under the same condition with the increasing amount of MEP, indicating that the MEP could enhance the reactivity in the DER/MEP-DDM systems.

In order to further evaluate the specific curing behavior, Kissinger's (1)<sup>46,47</sup> and Ozawa's theories (2)<sup>46–48</sup> were utilized to calculate the activation energy ( $E_a$ ) of DER/MEP-DDM systems, using the following eqs 1 and 2

$$-\ln\left(\frac{q}{T_p^2}\right) = E_a/RT_p - \ln\left(\frac{AR}{E_a}\right) \quad (1)$$

$$-\ln q = -\frac{1.052E_a}{RT_p} + \ln\left(\frac{AE_a}{R}\right) - \ln F(x) - 5.331 \quad (2)$$

where  $q$  is the heating rate,  $T_p$  is the exothermic peak temperature,  $R$  is the gas constant,  $A$  is the pre-exponential factor, and  $F(x)$  is a conversion dependent term. The  $E_a$  can be obtained from the slope of the linear fitting plot of  $\ln(q/T_p^2)$  versus  $1/T_p$  based on Kissinger's method  $\ln(q)$  versus  $1/T_p$  based on Ozawa's method, as shown in Figure 3e,f. The detailed data are reported in Table 1: the results showed that both Kissinger and Ozawa's methods well agreed in terms of  $E_a$  of the epoxy systems. Apparently, the DER/MEP (9:1)-DDM had lower  $E_a$  than neat EP. However, the  $E_a$  of the epoxy systems displayed a slight enhancement with the increasing content of MEP, which could be attributed to the steric hindrance effects of DOPO and hindered mobility of molecular segments, leading to high  $E_a$ .<sup>49</sup>

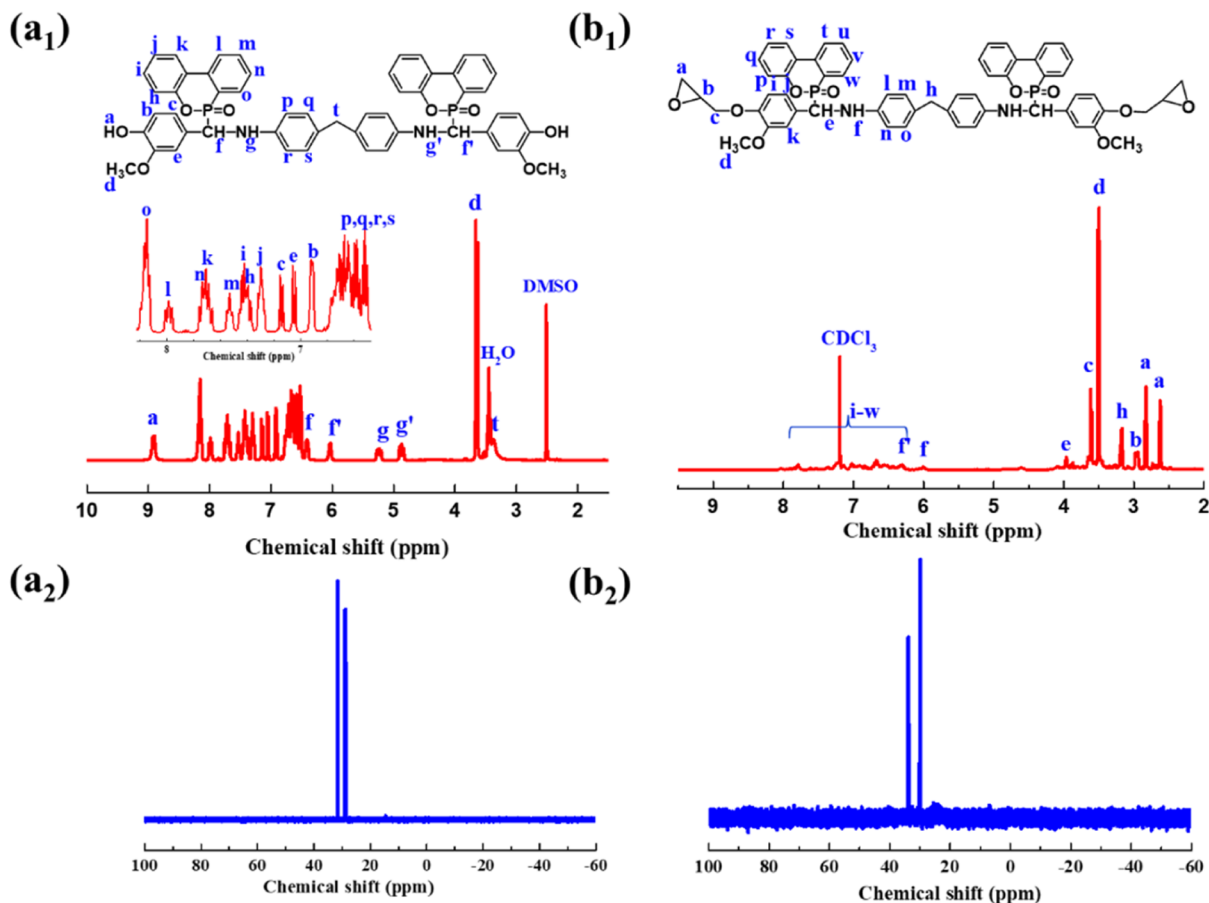


Figure 2.  $^1\text{H}$  NMR spectra of (a<sub>1</sub>) DN-bp and (b<sub>1</sub>) MEP and  $^{31}\text{P}$  NMR spectra of (a<sub>2</sub>) DN-bp and (b<sub>2</sub>) MEP.

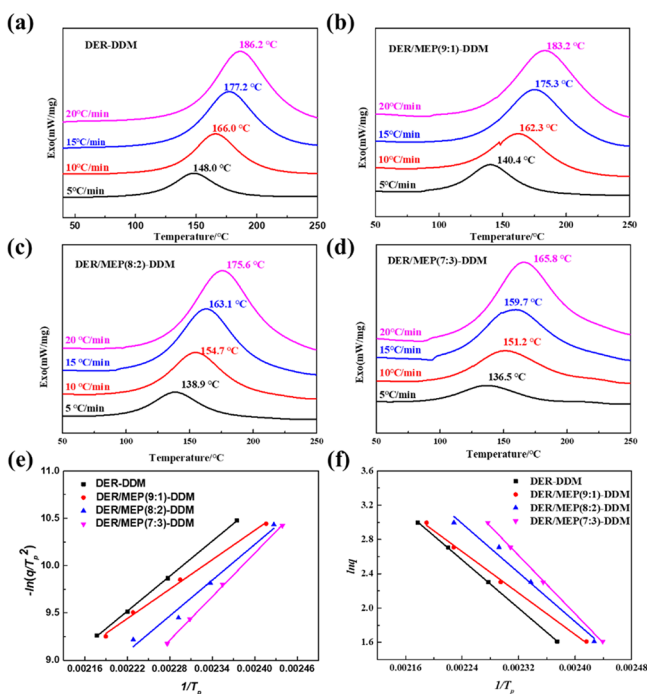


Figure 3. DSC curves for (a) DER-DDM, (b) DER/MEP (9:1)-DDM, (c) DER/MEP (8:2)-DDM, and (d) DER/MEP (7:3)-DDM at various heating rates; the related fitting curves of DER/MEP-DDM systems based on (e) Kissinger's and (f) Ozawa's theory.

Table 1. Activation Energy ( $E_a$ ) of DER/MEP-DDM Epoxy Systems

samples	$E_a$ (KJ/mol)	
	Kissinger	Ozawa
DER-DDM	51.29	55.70
DER/MEP(9:1)-DDM	43.01	47.73
DER/MEP(8:2)-DDM	52.32	56.53
DER/MEP(7:3)-DDM	63.55	67.10

FTIR spectra of cured DER/MEP-DDM systems and the curing process of cured DER/MEP-DDM systems are shown in Figure 4 and Scheme 3. It can be observed that the epoxy group at  $905\text{ cm}^{-1}$  disappears, and a new peak at  $3100\text{--}3500\text{ cm}^{-1}$  belonging to the hydroxyl group arose, indicating that the epoxy systems have been completely cured.<sup>18</sup>

**3.3. Mechanical Properties and Glass-Transition Temperature.** Figure 5a–d and Table S2 show the flexural properties of DER/MEP-DDM systems. The flexural modulus and strength of EPs containing MEP had an obvious enhancement in comparison with neat EP. The flexural strength and modulus of cured DER-DDM were 72.8 MPa and 1.3 GPa, respectively. For DER/MEP (9:1)-DDM, DER/MEP (8:2)-DDM, and DER/MEP (7:3)-DDM, the flexural strength increased to 75.6, 84.1, and 90.3 MPa, while the flexural modulus reached 1.7, 2.0, and 2.8 GPa, respectively. Flexural strength and moduli were strengthened by 3.8, 15.5, and 24.0% and 30.8, 53.8, and 115.4%, respectively. Meanwhile, the elongation at break declined gradually. The results were mainly attributed to the rigidity of MEP and strong polar

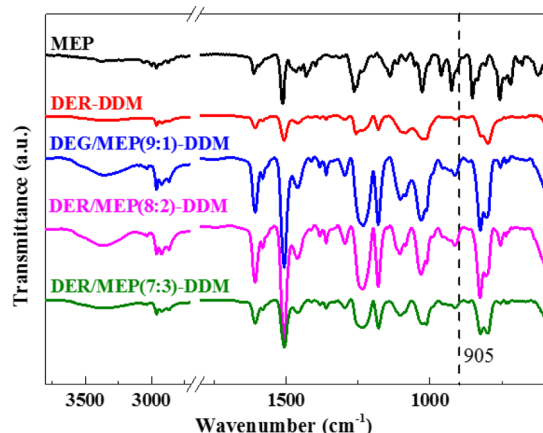


Figure 4. FTIR spectra of cured DER/MEP-DDM systems.

N–H resulted from intermolecular hydrogen bonds.<sup>50</sup> Flexural properties of epoxy resin MEP-DDM were less than satisfactory, probably because of highly steric hindrance of DOPO.<sup>51,52</sup>

Furthermore, the morphology of EPs exhibited a typical brittle fracture, as reported in Figure S4. The smooth fractured surface of all the samples demonstrated the good compatibility between MEP and DER. The  $T_g$  values of cured DER/MEP-DDM systems were determined by both DMA and DSC, and the  $T_g$  obtained from  $\tan \delta$  curves were slightly higher than those values measured by DSC, as visible in Figure 5e. It can be noted that the  $T_g$  decreased with the increasing amount of MEP, which was supposed to be related to the cross-linking density (Table S2).

**3.4. Flame Retardancy and Mechanism.** To visually investigate the flammability of DER/MEP-DDM systems, the UL-94 vertical combustion and LOI tests were carried out, and the data are presented in Figure 6a. The cured DER-DDM epoxy resin was burned out intensively with no rating in the

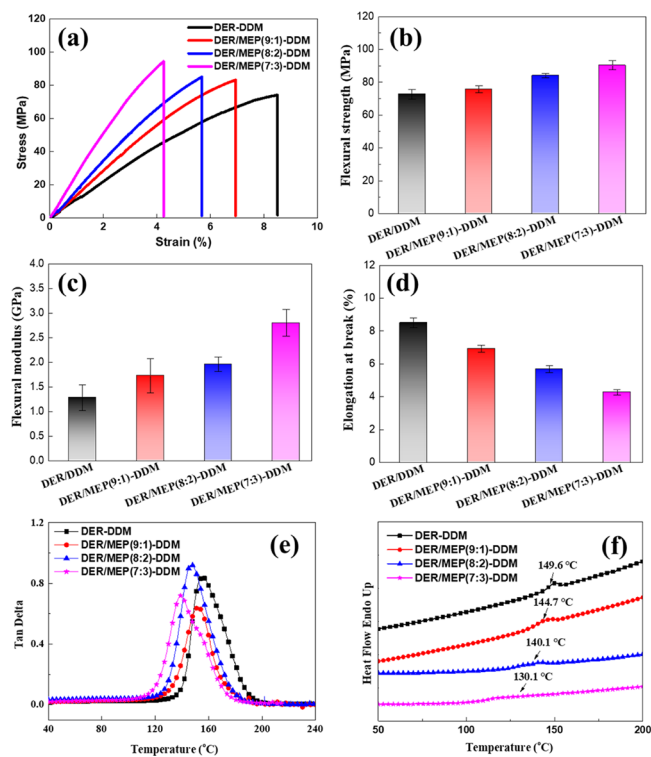
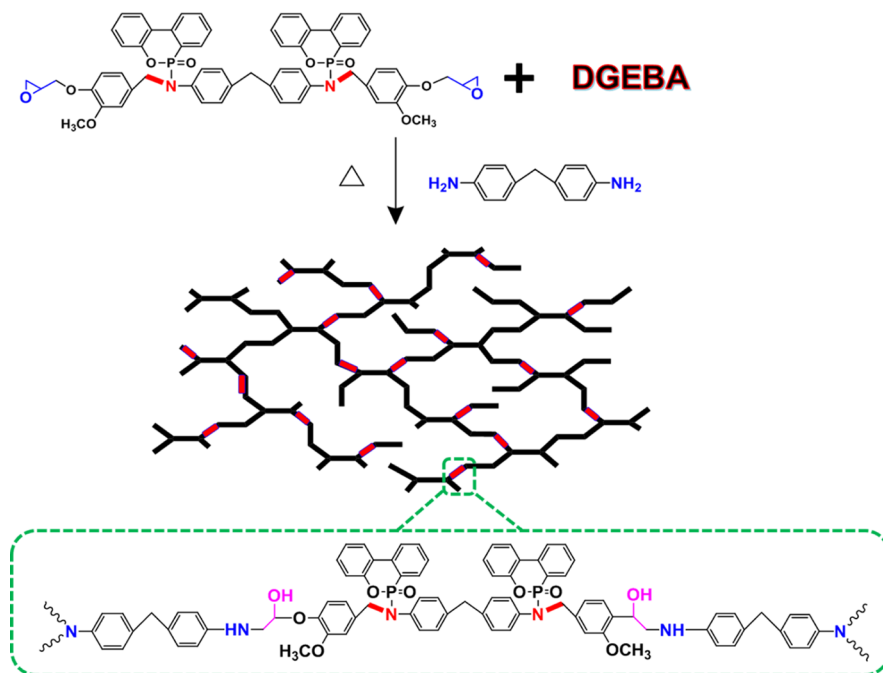
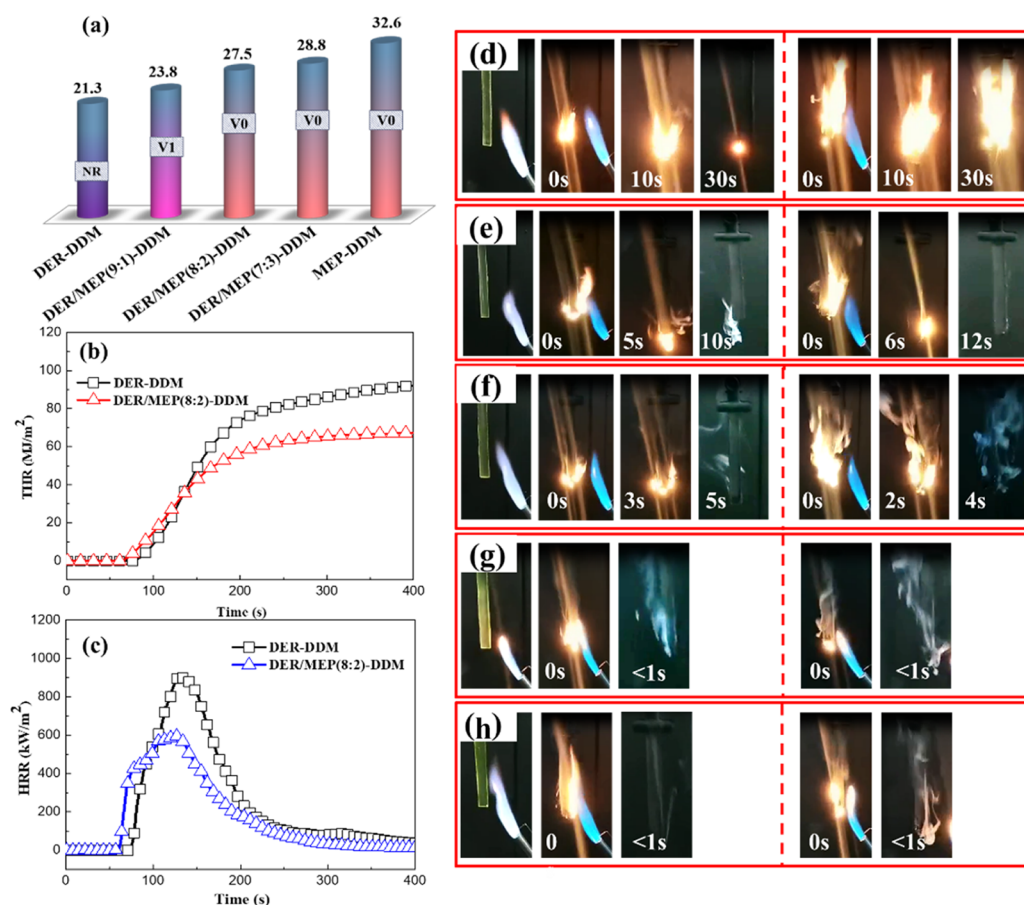


Figure 5. (a) Flexural stress–strain curves, (b) flexural strength, (c) flexural modulus, (d) elongation at break, (e)  $\tan \delta$  curves, and (f)  $T_g$  of cured DER/MEP-DDM systems.

UL-94 test (UL-94 NR), and it had a low LOI value of 21.3%. Nevertheless, the cured epoxy systems containing MEP exhibited small flames and self-extinguishing characteristics, as a result of gradual increase of LOI up to 28.8% for DER/MEP (7:3)-DDM. Besides, the LOI of neat MEP-DDM epoxy even reached 32.6%. For the UL-94 characterizations, the sample DER/MEP (9:1)-DDM (P w % = 0.52 wt %) could

### Scheme 3. Curing Process of Cured DER/MEP-DDM Systems





**Figure 6.** (a) LOI values of cured epoxy resins at different DER/MEP ratios; (b) THR and (c) HRR of cured DER-DDM and DER/MEP (8:2)-DDM epoxy resins; and digital photographs of vertical combustion of cured epoxy resins with various phosphorus-loading (d) DER-DDM; (e) DER/MEP (9:1)-DDM; (f) DER/MEP (8:2)-DDM; (g) DER/MEP (7:3)-DDM; and (h) MEP-DDM.

**Table 2. Results of the CCT for DER-DDM and DER/MEP (8:2)**

samples	PHRR (kW/m <sup>2</sup> )	THR (MJ/m <sup>2</sup> )	FGI (kW/(m <sup>2</sup> s))	Av-EHC(MJ/Kg)	char residue (%)
DER-DDM	911.4	92.7	6.9	24.859	15.2
DER/MEP(8:2)-DDM	594.8	67.6	4.6	19.391	19.6

self-extinguish within 10 s after igniting. More impressively, the flames of epoxy systems of both DER/MEP (8:2)-DDM and DER/MEP (7:3)-DDM, with P content of 1.06–1.62 wt %, become smaller and  $t_1 + t_2$  gradually reduced below 10 s. Importantly, the UL-94 test of these epoxy systems reached the V0 rating level. In addition, no flame droplets were seen during the combustion of all epoxy systems. The above phenomena demonstrated that the introduction of MEP could improve the flame retardancy performance of EPs.

The cone calorimetry test (CCT) is considered as the most representative method to evaluate the flame retardancy performance, owing to the simulated real combustion environment and continuous thermal radiation. Herein, DER/MEP (8:2)-DDM was taken as the representative example to analyze the flame retardancy performance. The results of total heat of release (THR), heat release rate (HRR), total smoke production (TSP), and char residue are given in Figures 6b,c and S5. The relevant detailed data are summarized in Tables 2 and S3. It was noted that the incorporation of MEP resulted in the higher and efficient flame retardancy effect. For instance, the THR of DER/MEP (8:2)-DDM was slumped from 92.7 to 67.6 MJ/m<sup>2</sup>, while the PHRR decreased from 911.4 to 594.8

kW/m<sup>2</sup>, displaying 27.1 and 34.7% reduction, respectively. Furthermore, the fire growth index (FGI, means the ratio of PHRR and time to PHRR) also decreased from 6.9 to 4.6 kW/(m<sup>2</sup>·s), demonstrating that the MEP impelled a high flame retardancy effect in epoxy systems. Effective heat of combustion (EHC) is a significant information in the combustion process, especially when the degree of combustion of volatiles in the gas phase has to be considered. As illustrated in Table 2, the DER/MEP (8:2)-DDM exhibited lower av-EHC than the DER-DDM, indicating that MEP could enhance the flame retardancy performance in the gas phase.<sup>53</sup> Furthermore, the averaged CO<sub>2</sub> production (av-CO<sub>2</sub>P) decreased and the av-COP (averaged CO production) increased (Table S3) due to quenching effect of PO•, PO<sub>2</sub>•, and phenoxy free radicals generated in the combustion process of the DOPO segment, resulting in incomplete combustion of volatiles.<sup>54,55</sup> Meanwhile, the TSP had a slight decrease, and the mass of the char residue enhanced by 28.9%. The synthesized EPs with a lower P content possessed excellent flame retardancy performance, which can be mainly due to the synergistic effect of P and N and the rigid benzene ring structure.

In order to investigate the morphology of the char residue in the condensed phase, the digital photographs and SEM images of epoxy systems after CCT are shown in Figure 7. It can be

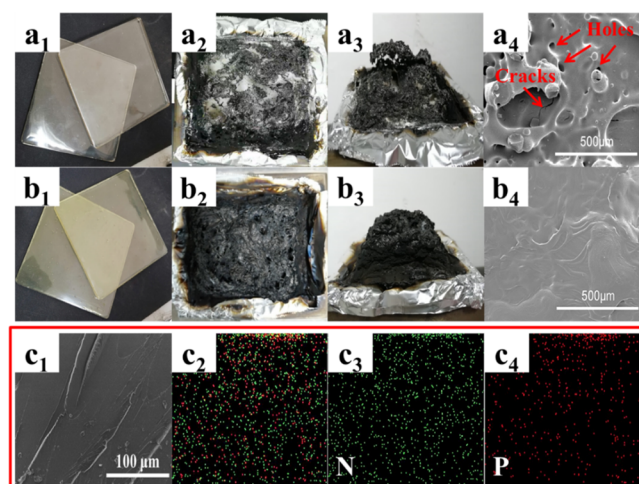
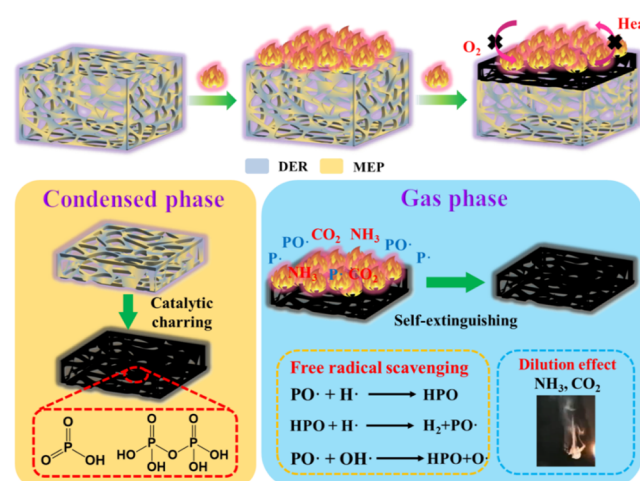


**Figure 7.** Digital photographs of DER-DDM ( $a_1$ ,  $a_2$ ,  $a_3$ ) and DER/MEP (8:2)-DDM ( $b_1$ ,  $b_2$ ,  $b_3$ ) before and after combustion, respectively; SEM images of DER-DDM ( $a_4$ ) and DER/MEP (8:2)-DDM ( $b_4$ ); and ( $c_1$ – $c_4$ ) SEM-assisted EDS mapping images of DER/MEP (8:2)-DDM.

observed that the char residue of DER-DDM epoxy resin exhibited discontinuous and loose morphology (Figure 7 $a_2$ ,  $a_3$ ), while the DER/MEP (8:2)-DDM showed more continuous and intact structure (Figure 7 $b_2$ ,  $b_3$ ). This phenomenon was due to the combustion of DOPO to produce phosphate, which is dehydrated with EP to form a protective char layer.<sup>56,57</sup> Additionally, SEM images of DER-DDM and DER/MEP (8:2)-DDM are reported in Figures 7 $a_4$ ,  $b_4$ . It can be clearly seen that DER-DDM showed some cavities and cracks on the surface that allow oxygen and heat to pass through the char layer, resulting in the poor flame retardancy performance. After incorporating MEP, the pores and cracks of the char layer of DER/MEP (8:2)-DDM were not observed, forming a dense char layer that could hinder the diffusion of oxygen and heat.<sup>43</sup> Therefore, the DER/MEP (8:2)-DDM epoxy resin showed lower THR, HRR, and PHRR than the neat epoxy. Meanwhile, the N and P elements were well distributed in the combusted DER/MEP (8:2)-DDM sample (Figure 7 $c_1$ – $c_4$ ).

Based on the above flame retardancy investigation and the dispersion of P and N elements by energy-dispersive system (EDS), the possible flame retardancy mechanisms of DER/MEP-DDM are illustrated in Scheme 4. In the gas phase, some free radicals containing phosphorus ( $PO\bullet$  and  $PO_2\bullet$ ) can capture activity of free radicals such as  $H\bullet$  and  $OH\bullet$  to intercept the chain radical reaction, thus extinguishing the flame. Besides, some nonflammable gases ( $CO_2$ ,  $NH_3$ , and  $H_2O$ ) generated by the DER/MEP-DDM can dilute flammable gases and result in self-extinguishing behavior of the epoxy matrix.<sup>43,58</sup> In the condensed phase, the formed pyrophosphoric acid and metaphosphoric acid by pyrolysis of the DOPO segment can promote carbonization of EPs to enhance the formation of char protective layers and char residues.<sup>13,26</sup> The synergistic effect of P and N also could improve the flame resistance efficiency because of the retarding volatilization effect of phosphoric acid by nitrogen-containing compound.

**Scheme 4.** Schematic Diagram of the Flame Retardancy Mechanism of EP



### 3.5. Flame-Retardant Epoxy/Graphene Composites with High Thermal Conductivity.

In order to expand the application of our vanillin-based EP, herein, intrinsic flame-retardant epoxy/graphene composites with high thermal conductivity were designed and fabricated. The detailed fabrication processes and the morphologies of the GA network and epoxy/GA composites are presented in the Supporting Information. DER/MEP (8:2)-DDM could be smoothly inserted into the GA network, due to the low viscosity as commercial epoxy at preheating temperature (Figure S6). In Figure 8, it can be seen that the DER-DDM/GA composites

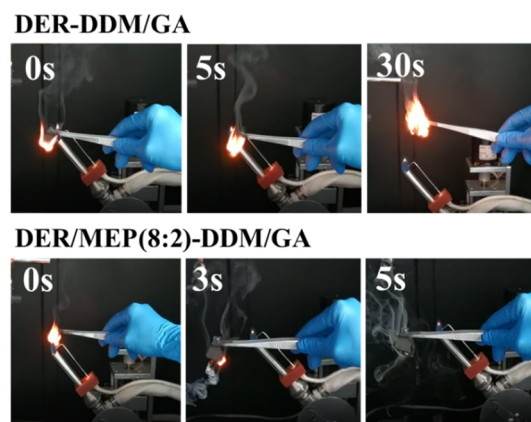


**Figure 8.** Combustion behaviors of epoxy/GA composites.

burn heavily after ignition for 10 s, and the flame did not expire after 30 s. On the other hand, the flame of the DER/MEP (8:2)-DDM/GA composite gradually abated and self-extinguished within 5 s, highlighting an impressive flame retardancy property.

As shown in Table 3, the density of GA is only  $6.3 \text{ mg}\cdot\text{cm}^{-3}$ , nonetheless increased significantly after being impregnated with epoxy, indicating a satisfactory connection between EP and GA after vacuum impregnation. The mass ratio of GA in the EP/GA composite was about 0.5%. The thermal conductivity ( $\lambda$ ) value of neat epoxy was about  $0.184 \text{ W}/(\text{m}\cdot\text{K})$ , which was consistent with the literatures.<sup>67,68</sup> The  $\lambda$  of EP/GA composites ranged from 0.49 to  $0.60 \text{ W}/(\text{m}\cdot\text{K})$ , which was higher than that of neat epoxy. It should be noted that  $\lambda$  values

Table 3. Thermal Conductivity Parameters of the EP/GA Composites<sup>a</sup>

samples	GA	EP <sub>1</sub>	EP <sub>2</sub>	EP <sub>1</sub> /GA	EP <sub>2</sub> /GA
$\rho$ /(mg·cm <sup>-3</sup> )	6.30	1120	1130	1065	1117
$\alpha$ (mm <sup>2</sup> /s)	NA	0.097	0.101	0.183	0.178
$\lambda$ (W/(m·K))	NA	0.184	0.193	0.493	0.592

<sup>a</sup>Note: the cured DER-DDM is EP<sub>1</sub>, and DER/MEP (8:2)-DDM is EP<sub>2</sub>.

of EP<sub>2</sub>/GA were slightly higher than EP<sub>1</sub>/GA, due to the higher  $\rho$  (density) and  $C_p$  (specific heat) for EP<sub>2</sub> than EP<sub>1</sub>. In order to eliminate the influence of the graphene content on  $\lambda$ , the thermal conductivity enhancement equation was used to express the thermal conductivity efficiency ( $\lambda_e$ ) when adding 1 vol % or 1 wt % of the thermally conductive filler, as follows

$$\lambda_e = (\lambda - \lambda_m) / w_f \lambda_m \quad (3)$$

where  $\lambda$  is the thermal conductivity of the composites,  $\lambda_m$  is the thermal conductivity of the matrix, and  $w_f$  represents the mass fraction of the filler.<sup>59</sup> In this work, the  $\lambda_e$  values of EP<sub>2</sub>/GA composites were compared with other graphene-based nanocomposites in the literatures,<sup>59–66</sup> as shown in Figure 9. EP<sub>2</sub>/GA composites in our work exhibited a higher  $\lambda_e$  value (409%).

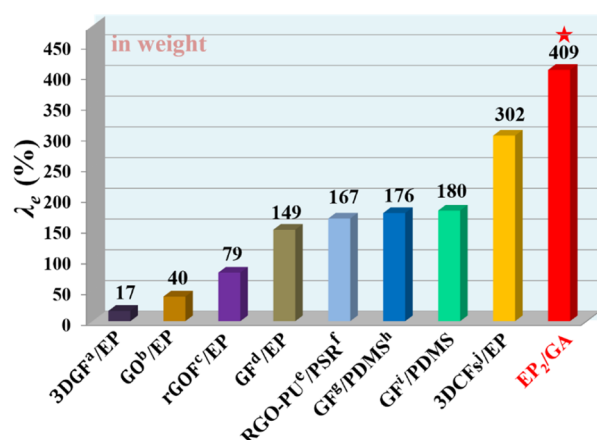


Figure 9. Comparison of  $\lambda_e$  of compositions with some representative publications.<sup>59–66</sup>

## CONCLUSIONS

Herein, intrinsically flame-retardant and thermal-conductive vanillin-based epoxy/GA composites were designed. First, a biobased intrinsic flame-retardant EP was realized by coupling vanillin with DDM and DOPO. The different amounts of MEP and DER were cured with DDM. The MEP can simultaneously enhance the flexural properties and flame retardancy performance of the epoxies. Due to the rigidity of MEP and strong intermolecular N–H hydrogen bonding interactions, flexural strength and modulus of DER/MEP (7:3)-DDM were improved by 24.0% and 115% compared to traditional EP. With a low P loading of 1.06 wt %, the DER/MEP (8:2)-DDM system reached UL-94 V0 rating and 27.5% of the LOI value. Besides, the THR and PHRR declined by 27 and 35%, respectively. The flame retardancy performance of DER/MEP-DDM was mainly attributed to the quenching effect with free radicals PO• and PO<sub>2</sub>•, nonflammable gas dilution effect, and the protective char layer, which hindered the heat/oxygen diffusion. Flame-retardant epoxy/graphene composites were

prepared by impregnating the epoxy into GAs. The epoxy composites exhibited excellent flame retardancy and thermal conductivity [ $\lambda = 0.592$  W/(m·K),  $\lambda_e = 409\%$ ] with only 0.5 wt % of graphene loading, ascribing this behavior to the integrated 3D graphene conductive pathways. We believe that this work would represent a novel solution for the preparation of high-performance biobased flame-retardant EP.

## ASSOCIATED CONTENT

### Supporting Information

The Supporting Information is available free of charge at <https://pubs.acs.org/doi/10.1021/acsami.1c19727>.

Preparation of 3D GA networks and EP/GA composites; characterizations; preparation process for GA and EP/GA composites; <sup>13</sup>C NMR spectra of DN-bp and MEP; TGA and DTG curves of cured DER/MEP-DDM systems; SEM images of the fractured surface of cured DER/MEP-DDM systems [DER-DDM; DER/MEP (9:1)-DDM; DER/MEP (8:2)-DDM; and DER/MEP (7:3)-DDM] ( $x = a, b, c, d$ ;  $x_1$  and  $x_2$  referring to the same sample observed at different magnifications); CCT curves of cured epoxy TSP; mass versus time; viscosity–temperature curves of DER, MEP, and DER/MEP(8:2) epoxy monomer; SEM images of GA; impact fractured surface of cured EP/GA composites EP<sub>1</sub>/GA and EP<sub>2</sub>/GA; GA and EP/GA composites (10 × 10 × 2 mm) [ $x = a$  (GA),  $b$  (EP<sub>1</sub>/GA),  $c$  (EP<sub>2</sub>/GA), where  $x$  and  $x'$  referring to different magnifications of the same sample]; formulations of cured epoxy systems; thermal and mechanical properties of cured epoxy resins; and specific parameters for DER-DDM and DER/MEP (8:2)-DDM obtained from the CCT (PDF)

## AUTHOR INFORMATION

### Corresponding Authors

**Weijun Yang** – The Key Laboratory of Synthetic and Biological Colloids, Ministry of Education, School of Chemical and Material Engineering, Jiangnan University, Wuxi 214122, China; [orcid.org/0000-0003-1810-8960](https://orcid.org/0000-0003-1810-8960); Email: [weijun.yang@jiangnan.edu.cn](mailto:weijun.yang@jiangnan.edu.cn)

**Piming Ma** – The Key Laboratory of Synthetic and Biological Colloids, Ministry of Education, School of Chemical and Material Engineering, Jiangnan University, Wuxi 214122, China; [orcid.org/0000-0002-4597-0639](https://orcid.org/0000-0002-4597-0639); Email: [p.ma@jiangnan.edu.cn](mailto:p.ma@jiangnan.edu.cn)

### Authors

**Hui Ding** – The Key Laboratory of Synthetic and Biological Colloids, Ministry of Education, School of Chemical and Material Engineering, Jiangnan University, Wuxi 214122, China

**Tianxi Liu** – The Key Laboratory of Synthetic and Biological Colloids, Ministry of Education, School of Chemical and Material Engineering, Jiangnan University, Wuxi 214122, China

**Rongxian Ou** – Key Laboratory for Biobased Materials and Energy of Ministry of Education, College of Materials and Energy, South China Agricultural University, Guangzhou 510642, China

**Jieying Lin** – The Key Laboratory of Synthetic and Biological Colloids, Ministry of Education, School of Chemical and Material Engineering, Jiangnan University, Wuxi 214122, China

**Debora Puglia** – Civil and Environmental Engineering Department, Materials Engineering Center, Perugia University, Terni 05100, Italy; [orcid.org/0000-0001-8515-7813](https://orcid.org/0000-0001-8515-7813)

**Pengwu Xu** – The Key Laboratory of Synthetic and Biological Colloids, Ministry of Education, School of Chemical and Material Engineering, Jiangnan University, Wuxi 214122, China; [orcid.org/0000-0001-7094-1445](https://orcid.org/0000-0001-7094-1445)

**Qingwen Wang** – Key Laboratory for Biobased Materials and Energy of Ministry of Education, College of Materials and Energy, South China Agricultural University, Guangzhou 510642, China

**Weifu Dong** – The Key Laboratory of Synthetic and Biological Colloids, Ministry of Education, School of Chemical and Material Engineering, Jiangnan University, Wuxi 214122, China; [orcid.org/0000-0002-7432-8362](https://orcid.org/0000-0002-7432-8362)

**Mingliang Du** – The Key Laboratory of Synthetic and Biological Colloids, Ministry of Education, School of Chemical and Material Engineering, Jiangnan University, Wuxi 214122, China; [orcid.org/0000-0003-2476-8594](https://orcid.org/0000-0003-2476-8594)

Complete contact information is available at:  
<https://pubs.acs.org/10.1021/acsami.1c19727>

## Notes

The authors declare no competing financial interest.

## ACKNOWLEDGMENTS

This work was financially supported by the National Science Foundation of China (51903106 and 51873082), the Distinguished Young Natural Science Foundation of Jiangsu Province (BK20200027), and the MOE & SAFEA 111 Project (B13025).

## REFERENCES

- (1) Zheng, N.; Huang, Y.; Liu, H.-Y.; Gao, J.; Mai, Y.-W. Improvement of Interlaminar Fracture Toughness in Carbon Fiber/Epoxy Composites with Carbon Nanotubes/Polysulfone Interleaves. *Compos. Sci. Technol.* **2017**, *140*, 8–15.
- (2) Guo, Y.; Chen, S.; Sun, L.; Yang, L.; Zhang, L.; Lou, J.; You, Z. Degradable and Fully Recyclable Dynamic Thermoset Elastomer for 3D-Printed Wearable Electronics. *Adv. Funct. Mater.* **2021**, *31*, 2009799–2009806.
- (3) Wang, S.; Fu, D.; Wang, X.; Pu, W.; Martone, A.; Lu, X.; Lavorgna, M.; Wang, Z.; Amendola, E.; Xia, H. High Performance Dynamic Covalent Crosslinked Polyacrylamide Composites with Self-Healing and Recycling Capabilities. *J. Mater. Chem. A* **2021**, *9*, 4055–4065.
- (4) Smith, R. J.; Holder, K. M.; Ruiz, S.; Hahn, W.; Song, Y.; Lvov, Y. M.; Grunlan, J. C. Environmentally Benign Halloysite Nanotube Multilayer Assembly Significantly Reduces Polyurethane Flammability. *Adv. Funct. Mater.* **2018**, *28*, 1703289–1703297.
- (5) Ai, Y.-F.; Xia, L.; Pang, F.-Q.; Xu, Y.-L.; Zhao, H.-B.; Jian, R.-K. Mechanically Strong and Flame-Retardant Epoxy Resins with Anti-Corrosion Performance. *Composites, Part B* **2020**, *193*, 108019–108031.

(6) Auvergne, R.; Caillol, S.; David, G.; Boutevin, B.; Pascault, J.-P. Biobased Thermosetting Epoxy: Present and Future. *Chem. Rev.* **2014**, *114*, 1082–1115.

(7) Wan, J.; Zhao, J.; Zhang, X.; Fan, H.; Zhang, J.; Hu, D.; Jin, P.; Wang, D.-Y. Epoxy Thermosets and Materials Derived from Bio-Based Monomeric Phenols: Transformations and Performances. *Prog. Polym. Sci.* **2020**, *108*, 101287–101333.

(8) Zhao, X.-L.; Liu, Y.-Y.; Weng, Y.; Li, Y.-D.; Zeng, J.-B. Sustainable Epoxy Vitrimers from Epoxidized Soybean Oil and Vanillin. *ACS Sustainable Chem. Eng.* **2020**, *8*, 15020–15029.

(9) Liu, Y.-Y.; He, J.; Li, Y.-D.; Zhao, X.-L.; Zeng, J.-B. Biobased Epoxy Vitriimer from Epoxidized Soybean Oil for Reprocessable and Recyclable Carbon Fiber Reinforced Composite. *Compos. Commun.* **2020**, *22*, 100445–100451.

(10) Miao, J.-T.; Peng, S.; Ge, M.; Li, Y.; Zhong, J.; Weng, Z.; Wu, L.; Zheng, L. Three-Dimensional Printing Fully Biobased Heat-Resistant Photoactive Acrylates from Aliphatic Biomass. *ACS Sustainable Chem. Eng.* **2020**, *8*, 9415–9424.

(11) Jia, P.; Zheng, M.; Ma, Y.; Feng, G.; Xia, H.; Hu, L.; Zhang, M.; Zhou, Y. Clean Synthesis of Epoxy Plasticizer with Quaternary Ammonium Phosphotungstate as Catalyst from a Byproduct of Cashew Nut Processing. *J. Clean. Prod.* **2019**, *206*, 838–849.

(12) Wu, H.; Liu, C.; Cheng, L.; Yu, Y.; Zhao, H.; Wang, L. Enhancing the mechanical and tribological properties of epoxy composites via incorporation of reactive bio-based epoxy functionalized graphene oxide. *RSC Adv.* **2020**, *10*, 40148–40156.

(13) Huo, S.; Song, P.; Yu, B.; Ran, S.; Chevali, V. S.; Liu, L.; Fang, Z.; Wang, H. Phosphorus-Containing Flame Retardant Epoxy Thermosets: Recent Advances and Future Perspectives. *Prog. Polym. Sci.* **2021**, *114*, 101366–101402.

(14) Van De Pas, D. J.; Torr, K. M. Biobased Epoxy Resins from Deconstructed Native Softwood Lignin. *Biomacromolecules* **2017**, *18*, 2640–2648.

(15) Yang, W.; Xu, F.; Ma, X.; Guo, J.; Li, C.; Shen, S.; Puglia, D.; Chen, J.; Xu, P.; Kenny, J.; Ma, P. Highly-Toughened PVA/Nanocellulose Hydrogels with Anti-Oxidative and Antibacterial Properties Triggered by Lignin-Ag Nanoparticles. *Mater. Sci. Eng. C* **2021**, *129*, 112385.

(16) Yang, W.; Ding, H.; Qi, G.; Guo, J.; Xu, F.; Li, C.; Puglia, D.; Kenny, J.; Ma, P. Enhancing the Radical Scavenging Activity and UV Resistance of Lignin Nanoparticles via Surface Mannich Amination toward a Biobased Antioxidant. *Biomacromolecules* **2021**, *22*, 2693–2701.

(17) Qi, Y.; Weng, Z.; Kou, Y.; Song, L.; Li, J.; Wang, J.; Zhang, S.; Liu, C.; Jian, X. Synthesize and Introduce Bio-Based Aromatic s-Triazine in Epoxy Resin: Enabling Extremely High Thermal Stability, Mechanical Properties, and Flame Retardancy to Achieve High-Performance Sustainable Polymers. *Chem. Eng. J.* **2021**, *406*, 126881–126893.

(18) Wang, S.; Ma, S.; Xu, C.; Liu, Y.; Dai, J.; Wang, Z.; Liu, X.; Chen, J.; Shen, X.; Wei, J.; Zhu, J. Vanillin-Derived High-Performance Flame Retardant Epoxy Resins: Facile Synthesis and Properties. *Macromolecules* **2017**, *50*, 1892–1901.

(19) De Kruijff, G. H. M.; Goschler, T.; Beiser, N.; Stenglein, A.; Türk, O. M.; Waldvogel, S. R. Sustainable Access to Biobased Biphenol Epoxy Resins by Electrochemical Dehydrogenative Dimerization of Eugenol. *Green Chem.* **2019**, *21*, 4815–4823.

(20) Kim, H.; Kim, D. W.; Vasagar, V.; Ha, H.; Nazarenko, S.; Ellison, C. J. Polydopamine-Graphene Oxide Flame Retardant Nanocoatings Applied via an Aqueous Liquid Crystalline Scaffold. *Adv. Funct. Mater.* **2018**, *28*, 1803172–1803181.

(21) Cai, W.; Wang, J.; Pan, Y.; Guo, W.; Mu, X.; Feng, X.; Yuan, B.; Wang, X.; Hu, Y. Mussel-Inspired Functionalization of Electrochemically Exfoliated Graphene: Based on Self-Polymerization of Dopamine and Its Suppression Effect on the Fire Hazards and Smoke Toxicity of Thermoplastic Polyurethane. *J. Hazard. Mater.* **2018**, *352*, 57–69.

(22) Cai, W.; Cai, T.; He, L.; Chu, F.; Mu, X.; Han, L.; Hu, Y.; Wang, B.; Hu, W. Natural Antioxidant Functionalization for Fabricating Ambient-Stable Black Phosphorus Nanosheets toward

Enhancing Flame Retardancy and Toxic Gases Suppression of Polyurethane. *J. Hazard. Mater.* **2020**, *387*, 121971–121984.

(23) Faye, I.; Decostanzi, M.; Ecochard, Y.; Caillol, S. Eugenol Bio-Based Epoxy Thermosets: From Cloves to Applied Materials. *Green Chem.* **2017**, *19*, 5236–5242.

(24) Shi, Y.-Q.; Fu, T.; Xu, Y.-J.; Li, D.-F.; Wang, X.-L.; Wang, Y.-Z. Novel Phosphorus-Containing Halogen-Free Ionic Liquid toward Fire Safety Epoxy Resin with Well-Balanced Comprehensive Performance. *Chem. Eng. J.* **2018**, *354*, 208–219.

(25) Yang, H.; Yu, B.; Xu, X.; Bourbigot, S.; Wang, H.; Song, P. Lignin-Derived Bio-Based Flame Retardants toward High-Performance Sustainable Polymeric Materials. *Green Chem.* **2020**, *22*, 2129–2161.

(26) Liu, T.; Sun, L.; Ou, R.; Fan, Q.; Li, L.; Guo, C.; Liu, Z.; Wang, Q. Flame Retardant Eugenol-Based Thiol-Ene Polymer Networks with High Mechanical Strength and Transparency. *Chem. Eng. J.* **2019**, *368*, 359–368.

(27) Ma, C.; Yu, B.; Hong, N.; Pan, Y.; Hu, W.; Hu, Y. Facile Synthesis of a Highly Efficient, Halogen-Free, and Intumescent Flame Retardant for Epoxy Resins: Thermal Properties, Combustion Behaviors, and Flame-Retardant Mechanisms. *Ind. Eng. Chem. Res.* **2016**, *55*, 10868–10879.

(28) Guo, W.; Wang, X.; Huang, J.; Cai, W.; Song, L.; Hu, Y. Intrinsically Anti-Flammable and Self-Toughened Phosphorylated Cardanol-Derived Novolac Epoxy Thermosets. *Ind. Crops Prod.* **2021**, *166*, 113496–113508.

(29) Gnanasekar, P.; Chen, H.; Tratnik, N.; Feng, M.; Yan, N. Enhancing performance of phosphorus containing vanillin-based epoxy resins by P-N non-covalently functionalized graphene oxide nanofillers. *Composites, Part B* **2021**, *207*, 108585–108597.

(30) Gnanasekar, P.; Feng, M.; Yan, N. Facile Synthesis of a Phosphorus-Containing Sustainable Biomolecular Platform from Vanillin for the Production of Mechanically Strong and Highly Flame-Retardant Resins. *ACS Sustainable Chem. Eng.* **2020**, *8*, 17417–17426.

(31) Fang, Z.; Nikafshar, S.; Hegg, E. L.; Nejad, M. Biobased Divanillin As a Precursor for Formulating Biobased Epoxy Resin. *ACS Sustainable Chem. Eng.* **2020**, *8*, 9095–9103.

(32) Zhang, Y.; Jing, J.; Liu, T.; Xi, L.; Sai, T.; Ran, S.; Fang, Z.; Huo, S.; Song, P. A Molecularly Engineered Bioderived Polyphosphate for Enhanced Flame Retardant, UV-Blocking and Mechanical Properties of Poly(Lactic Acid). *Chem. Eng. J.* **2021**, *411*, 128493–128506.

(33) Meng, J.; Chen, P.; Yang, R.; Dai, L.; Yao, C.; Fang, Z.; Guo, K. Thermal Stable Honokiol-Derived Epoxy Resin with Reinforced Thermal Conductivity, Dielectric Properties and Flame Resistance. *Chem. Eng. J.* **2021**, *412*, 128647–128659.

(34) Qi, Y.; Wang, J.; Kou, Y.; Pang, H.; Zhang, S.; Li, N.; Liu, C.; Weng, Z.; Jian, X. Synthesis of an Aromatic N-Heterocycle Derived from Biomass and Its Use as a Polymer Feedstock. *Nat. Commun.* **2019**, *10*, 1–9.

(35) Guo, W.; Zhao, Y.; Wang, X.; Cai, W.; Wang, J.; Song, L.; Hu, Y. Multifunctional Epoxy Composites with Highly Flame Retardant and Effective Electromagnetic Interference Shielding Performances. *Composites, Part B* **2020**, *192*, 107990.

(36) Li, Z.; Lei, S.; Xi, J.; Ye, D.; Hu, W.; Song, L.; Hu, Y.; Cai, W.; Gui, Z. Bio-Based Multifunctional Carbon Aerogels from Sugarcane Residue for Organic Solvents Adsorption and Solar-Thermal-Driven Oil Removal. *Chem. Eng. J.* **2021**, *426*, 129580–129592.

(37) Feng, Y.; Han, G.; Wang, B.; Zhou, X.; Ma, J.; Ye, Y.; Liu, C.; Xie, X. Multiple Synergistic Effects of Graphene-Based Hybrid and Hexagonal Born Nitride in Enhancing Thermal Conductivity and Flame Retardancy of Epoxy. *Chem. Eng. J.* **2020**, *379*, 122402–122415.

(38) Wang, X.; Kalali, E. N.; Wan, J.-T.; Wang, D.-Y. Carbon-Family Materials for Flame Retardant Polymeric Materials. *Prog. Polym. Sci.* **2017**, *69*, 22–46.

(39) Gu, J.; Liang, C.; Zhao, X.; Gan, B.; Qiu, H.; Guo, Y.; Yang, X.; Zhang, Q.; Wang, D.-Y. Highly Thermally Conductive Flame-

Retardant Epoxy Nanocomposites with Reduced Ignitability and Excellent Electrical Conductivities. *Compos. Sci. Technol.* **2017**, *139*, 83–89.

(40) Feng, Y.; Li, X.; Zhao, X.; Ye, Y.; Zhou, X.; Liu, H.; Liu, C.; Xie, X. Synergetic Improvement in Thermal Conductivity and Flame Retardancy of Epoxy/Silver Nanowires Composites by Incorporating "Branch-Like" Flame-Retardant Functionalized Graphene. *ACS Appl. Mater. Interfaces* **2018**, *10*, 21628–21641.

(41) Liu, T.; Hao, C.; Zhang, S.; Yang, X.; Wang, L.; Han, J.; Li, Y.; Xin, J.; Zhang, J. A Self-Healable High Glass Transition Temperature Bioepoxy Material Based on Vitrimer Chemistry. *Macromolecules* **2018**, *51*, 5577–5585.

(42) Chi, Z.; Guo, Z.; Xu, Z.; Zhang, M.; Li, M.; Shang, L.; Ao, Y. A DOPO-Based Phosphorus-Nitrogen Flame Retardant Bio-Based Epoxy Resin from Diphenolic Acid: Synthesis, Flame-Retardant Behavior and Mechanism. *Polym. Degrad. Stab.* **2020**, *176*, 109151–109165.

(43) Chen, Y.; Duan, H.; Ji, S.; Ma, H. Novel Phosphorus/Nitrogen/Boron-Containing Carboxylic Acid as Co-Curing Agent for Fire Safety of Epoxy Resin with Enhanced Mechanical Properties. *J. Hazard. Mater.* **2021**, *402*, 123769–123781.

(44) Liu, C.; Chen, T.; Yuan, C. H.; Song, C. F.; Chang, Y.; Chen, G. R.; Xu, Y. T.; Dai, L. Z. Modification of Epoxy Resin through the Self-Assembly of a Surfactant-like Multi-Element Flame Retardant. *J. Mater. Chem. A* **2016**, *4*, 3462–3470.

(45) Ma, S.; Liu, X.; Jiang, Y.; Tang, Z.; Zhang, C.; Zhu, J. Bio-Based Epoxy Resin from Itaconic Acid and Its Thermosets Cured with Anhydride and Comonomers. *Green Chem.* **2013**, *15*, 245–254.

(46) Liu, J.; Dai, J.; Wang, S.; Peng, Y.; Cao, L.; Liu, X. Facile Synthesis of Bio-Based Reactive Flame Retardant from Vanillin and Guaiacol for Epoxy Resin. *Composites, Part B* **2020**, *190*, 107926–107939.

(47) Mashouf Roudsari, G.; Mohanty, A. K.; Misra, M. Study of the Curing Kinetics of Epoxy Resins with Biobased Hardener and Epoxidized Soybean Oil. *ACS Sustainable Chem. Eng.* **2014**, *2*, 2111–2116.

(48) Tan, Y.; Shao, Z.-B.; Chen, X.-F.; Long, J.-W.; Chen, L.; Wang, Y.-Z. Novel Multifunctional Organic-Inorganic Hybrid Curing Agent with High Flame-Retardant Efficiency for Epoxy Resin. *ACS Appl. Mater. Interfaces* **2015**, *7*, 17919–17928.

(49) Liu, H.; Wang, X.; Wu, D. Novel Cyclotriphosphazene-Based Epoxy Compound and Its Application in Halogen-Free Epoxy Thermosetting Systems: Synthesis, Curing Behaviors, and Flame Retardancy. *Polym. Degrad. Stab.* **2014**, *103*, 96–112.

(50) Liu, H.; Xu, K.; Cai, H.; Su, J.; Liu, X.; Fu, Z.; Chen, M. Thermal Properties and Flame Retardancy of Novel Epoxy Based on Phosphorus-Modified Schiff-Base. *Polym. Adv. Technol.* **2012**, *23*, 114–121.

(51) Zou, J.; Duan, H.; Chen, Y.; Ji, S.; Cao, J.; Ma, H. A P/N/S-Containing High-Efficiency Flame Retardant Endowing Epoxy Resin with Excellent Flame Retardance, Mechanical Properties and Heat Resistance. *Composites, Part B* **2020**, *199*, 108228–108240.

(52) Zhao, P.; Rao, W.; Luo, H.; Wang, L.; Liu, Y.; Yu, C. Novel Organophosphorus Compound with Amine Groups towards Self-Extinguishing Epoxy Resins at Low Loading. *Mater. Des.* **2020**, *193*, 108838–108850.

(53) Wu, N.; Fu, G.; Yang, Y.; Xia, M.; Yun, H.; Wang, Q. Fire Safety Enhancement of a Highly Efficient Flame Retardant Poly-(Phenylphosphoryl Phenylenediamine) in Biodegradable Poly(Lactic Acid). *J. Hazard. Mater.* **2019**, *363*, 1–9.

(54) Cai, W.; Li, Z.; Mu, X.; He, L.; Zhou, X.; Guo, W.; Song, L.; Hu, Y. Barrier Function of Graphene for Suppressing the Smoke Toxicity of Polymer/Black Phosphorus Nanocomposites with Mechanism Change. *J. Hazard. Mater.* **2021**, *404*, 124106–124119.

(55) Xiao, Y.; Jin, Z.; He, L.; Ma, S.; Wang, C.; Mu, X.; Song, L. Synthesis of a Novel Graphene Conjugated Covalent Organic Framework Nanohybrid for Enhancing the Flame Retardancy and Mechanical Properties of Epoxy Resins through Synergistic Effect. *Composites, Part B* **2020**, *182*, 107616–107627.

(56) Li, X.; Zhang, J.; Zhang, L.; Ruiz de Luzuriaga, A.; Rekondo, A.; Wang, D.-Y. Recyclable Flame-Retardant Epoxy Composites Based on Disulfide Bonds: Flammability and Recyclability. *Compos. Commun.* **2021**, *25*, 100754–100761.

(57) Zhang, J.; Li, Z.; Yin, G.-Z.; Wang, D.-Y. Construction of a novel three-in-one biomass based intumescent fire retardant through phosphorus functionalized metal-organic framework and  $\beta$ -cyclodextrin hybrids in achieving fire safe epoxy. *Compos. Commun.* **2021**, *23*, 100594–100602.

(58) Cai, W.; Feng, X.; Wang, B.; Hu, W.; Yuan, B.; Hong, N.; Hu, Y. A Novel Strategy to Simultaneously Electrochemically Prepare and Functionalize Graphene with a Multifunctional Flame Retardant. *Chem. Eng. J.* **2017**, *316*, 514–524.

(59) Li, Y.; Wei, W.; Wang, Y.; Kadhim, N.; Mei, Y.; Zhou, Z. Construction of Highly Aligned Graphene-Based Aerogels and Their Epoxy Composites towards High Thermal Conductivity. *J. Mater. Chem. C* **2019**, *7*, 11783–11789.

(60) Zhou, H.; Wang, H.; Du, X.; Zhang, Y.; Zhou, H.; Yuan, H.; Liu, H.-Y.; Mai, Y.-W. Facile Fabrication of Large 3D Graphene Filler Modified Epoxy Composites with Improved Thermal Conduction and Tribological Performance. *Carbon* **2018**, *139*, 1168–1177.

(61) Zhou, H.; Wang, H.; Du, X.; Mo, Y.; Yuan, H.; Liu, H.-Y. Hybrid Three-Dimensional Graphene Fillers and Graphite Platelets to Improve the Thermal Conductivity and Wear Performance of Epoxy Composites. *Composites, Part A* **2019**, *123*, 270–277.

(62) Liu, Z.; Shen, D.; Yu, J.; Dai, W.; Li, C.; Du, S.; Jiang, N.; Li, H.; Lin, C.-T. Exceptionally High Thermal and Electrical Conductivity of Three-Dimensional Graphene-Foam-Based Polymer Composites. *RSC Adv.* **2016**, *6*, 22364–22369.

(63) Zhao, Y.-H.; Zhang, Y.-F.; Bai, S.-L. High Thermal Conductivity of Flexible Polymer Composites Due to Synergistic Effect of Multilayer Graphene Flakes and Graphene Foam. *Composites, Part A* **2016**, *85*, 148–155.

(64) Zhao, Y.-H.; Zhang, Y.-F.; Wu, Z.-K.; Bai, S.-L. Synergic Enhancement of Thermal Properties of Polymer Composites by Graphene Foam and Carbon Black. *Composites Part B* **2016**, *84*, 52–58.

(65) Tao, W.; Zeng, S.; Xu, Y.; Nie, W.; Zhou, Y.; Qin, P.; Wu, S.; Chen, P. 3D Graphene - sponge skeleton reinforced polysulfide rubber nanocomposites with improved electrical and thermal conductivity. *Composites, Part A* **2021**, *143*, 106293–106302.

(66) Zhang, C.; Shi, Z.; Li, A.; Zhang, Y.-F. RGO-Coated Polyurethane Foam/Segmented Polyurethane Composites as Solid-Solid Phase Change Thermal Interface Material. *Polymers* **2020**, *12*, 3004–3013.

(67) Samad, Y. A.; Li, Y.; Schiffer, A.; Alhassan, S. M.; Liao, K. Graphene Foam Developed with a Novel Two-Step Technique for Low and High Strains and Pressure-Sensing Applications. *Small* **2015**, *11*, 2380–2385.

(68) Shi, X.; Zhang, R.; Ruan, K.; Ma, T.; Guo, Y.; Gu, J. Improvement of Thermal Conductivities and Simulation Model for Glass Fabrics Reinforced Epoxy Laminated Composites via Introducing Hetero-Structured BNN-30@BNNS Fillers. *J. Mater. Sci. Technol.* **2021**, *82*, 239–249.